ELSEVIER

Contents lists available at ScienceDirect

Chemical Physics Impact

journal homepage: www.sciencedirect.com/journal/chemical-physics-impact



Full Length Article



Facile synthesis of Co₃O₄@SeNPs grafted MWCNTs Nanocomposite for high energy density supercapacitor and antimicrobial applications

Jothirathinam Thangarathinam ^a, Muthukrishnan Francklin Philips ^{a,*}, Violet Dhayabaran ^{a,*}, Bavatharani Chokkiah ^b, Jayakumar Princy ^a, Cyril Arockiaraj Crispin Tina ^a, Annadurai Kasthuri ^a, Ragupathy Dhanusuraman ^{b,*}

a P.G. and Research Department of Chemistry, Bishop Heber College (Autonomous), Affiliated to Bharathidasan University, Tiruchirappalli, 620 017, Tamil Nadu, India

ARTICLE INFO

Keywords: Multi-walled carbon nanotubes Thiol(-SH) functionalized MWCNTs Cobalt oxide nanoparticles Selenium nanoparticles Supercapacitor Antimicrobial activity

ABSTRACT

Herein for the first time, intertwined nanocomposite (Co3O4@Se NPs/MWCNTs) of cobalt oxide nanoparticles (Co3O4 NPs) adsorbed on selenium nanoparticles (Se NPs) (designated as Co3O4@Se NPs) and thiol (–SH) functionalized multiwalled carbon nanotubes (MWCNTs) was synthesized by a simple hydrothermal method to achieve excellent capacitive and microbicidal performance. The surface morphology, microstructure and functional group studies ensures that the existence of Co3O4@Se NPs onto MWCNTs. The electrochemical studies (cyclic voltammetry (CV), electrochemical impedance spectroscopy (EIS) and galvanostatic charge-discharge (GCD)) were performed and demonstrated the Supercapacitive performance of Co3O4@Se NPs/MWCNTs nanocomposite. Higher electrochemical capacitance (356 F/g) with better coulombic efficiency of 84% was acquired. Also, it exhibited an admirable antimicrobial study and illustrated that the pathogens were more susceptible to Co3O4@Se NPs/MWCNTs nanocomposite. The superior electrochemical and antimicrobial activity was achieved owing to the specific inherent properties of thiol (–SH) groups opt binding and stabilizing Co3O4@Se NPs against its aggregation on the surface of MWCNTs. The thiol (–SH) group influences the enrichment of Co3O4@Se NPs onto MWCNTs and facilitates in enhancement of energy storage and microbicidal performance the nanocomposite. These attained outcomes put forward the applicability of the synthesized active nanocomposite towards supercapacitor and antibacterial agents against pathogens.

1. Introduction

Thrust of emerging multifunctional materials have drawn huge interest in the research community. In that nanotechnology has gained tremendous interest in the active field of research owing to its remarkable potential for a variety of applications includes sensor, supercapacitor, fuel cell, antimicrobial activity, etc. which is acquired due to combine electrical, thermal, mechanical, and biological characteristics [1,2]. When the size of particles is reduced to nanoscale, the materials with radically improved or new surprising physicochemical features often emerge. Multi walled carbon nanotubes (MWCNTs) as important one-dimensional (1D) nanomaterials [3,4] have gained immense attention for their applications [5] in diversify fields due to its unique properties [6]. The excellent performance and spectacular applications of MWCNTs are pertaining to its dispersability in aqueous/ organic

phases [7,8]. However, the major obstacles of MWCNT to use as such are high Van der Waals force, surface area and high aspect ratio which cause self-aggregation and poor dispersability in aqueous/organic solvents [9, 10]. Hence, the strategies which could enhance de-agglomeration and uniform dispersion of MWCNTs are crucial to bring significant and expected outcomes [11,12]. The attachment of functional groups on the surface of MWCNTs through functionalization is an effective way to improve reactivity, provide active sites for further process, prevent aggregation and achieve better dispersion of MWCNTs [13,14]. The properties of functionalized MWCNT are expected to make the way toward nanotechnology applications [15,16]. The functionalization of MWCNTs can be achieved through both covalent and non-covalent approaches to impart solubility and chemical modifications to MWCNTs [17]. Surface functionalization of MWCNT through covalent bonding is the most preferred technique [18,19]. The covalent method of

E-mail addresses: francklin78@gmail.com (M.F. Philips), violetdhaya@gmail.com (V. Dhayabaran), ragu@nitpy.ac.in (R. Dhanusuraman).

b Nano Electrochemistry Lab (NEL), Department of Chemistry, National Institute of Technology Puducherry, Karaikal 609-609, India

^{*} Corresponding authors.

functionalization of MWCNT causes covalent linkages between functional groups and MWCNTs. It is one of the most promising methods of altering carbon nanomaterials through reactions either on the ends or sidewalls of nanotubes [20]. Covalent functionalization offers many outstanding physicochemical properties to MWCNTs such as improved interfacial adhesion, good adsorption efficiency, efficient solubility/dispersibility in aqueous/organic medium, minimization of aggregation and chemical interactions with other molecules (bio-molecule, polymer, inorganic., etc.) [21,22]. Various functional groups such as thiol (-SH), silane (-SiH₄), phenol (-OH), carboxyl (-COOH), poly(styrene-co-acrylonitrile) and amine (-NH2) were attached covalently onto MWCNT to improve its properties [23]. Among these functional groups, the thiol (-SH) group has gained tremendous interest in the field of materials science because of its inherent beneficial properties such as influence on morphology /microstructure, uniform distribution, stability/protection enrichment of nanoparticles on the surface of MWCNTs against agglomeration/leaching processes and performance of the prepared materials. A derivative of aniline, aminothiophenol, as a functionalized modified material, has been widely used in various fields [24,25]. Since thiol (-SH) group has an excellent anchoring/binding ability to nanoparticles (metal/metal oxide) through molecular interaction between thiol (-SH) group and nanoparticles [26, 27], the existence of such groups on the surface of MWCNTs have received keen interest among scientific community [28,29].

On the other hand, transition metal oxide have drawn much attention as a promising type of multifunctional materials [30–33], in specific such as cobalt oxide nanoparticles (Co₃O₄ NPs) due to their widespread applications in various fields such as environment, gas sensing, lithium-ion batteries, energy storage, magnetic semiconductors, pigments, catalysis, electrochromic devices, cosmetics, water treatment, antibacterial activity, etc. [34,35]. Recently, it has been demonstrated that Co₃O₄ NPs display antimicrobial activity against micro-organisms [36]. On the other hand, Co₃O₄ NPs exhibits high particle aggregation [37,12], which limits their reactive centers/sites leading to rapid capacity fading, low stability and poor performance. To overcome these demerits, it is necessary to incorporate Co₃O₄ NPs with high conductivity materials, such as conducting polymers, MWCNT and graphene [38]. MWCNT can facilitate charge transfer mechanism and provide stability to nanoparticles against aggregation process [39]. Nanosize Se NPs has aroused global interest in research due to its meritorious physico-chemical properties and excellent biological activities [40,41].

Based on the interdisciplinary research escalation and their significance [42], the synergistic combination of materials was chosen to enhance the energy storage and antimicrobial properties [43] in developing biocompatible, wearable energy storage devices applications [44]. Thus, in this present work a facile hydrothermal method was employed to synthesize Co₃O₄@Se NPs/MWCNTs nanocomposite. Electrochemical analysis was conducted in the developed nanocomposites and measured highest specific capacitance 356 F/g at 5 mV/sec. The antimicrobial activity of Co₃O₄@Se NPs/MWCNTs nanocomposite was studied against various microbes (Gram-negative (G-) bacteria and fungus). To the best of our understanding, there are no earlier reports on the synthesis of Co₃O₄@Se NPs/MWCNTs nanocomposite and its studies towards Supercapacitive performances as well as antimicrobial property. In addition to this, despite enormous amounts of individual reports available on the energy storage performances of Co₃O₄/MWCNT and the antimicrobial activity of both Co₃O₄ NPs and Se NPs, employment of nanocomposite comprising of both Co₃O₄ NPs and Se NPs as antibody to resist the growth of various pathogens is not addressed yet. The beneficial properties of thiol (-SH) groups have been properly exploited in effective anchoring and distribution of Co₃O₄@Se NPs onto MWCNTs. As a result, Co₃O₄@Se NPs/MWCNTs nanocomposite profound as a significantly active electrode material for supercapacitors and microbicidal effect towards micro-organisms.

2. Experimental

2.1. Materials and instruments

Multiwalled carbon nanotube (MWCNT, SRL), 2-amino thiophenol (2-ATP, Avra), thionyl chloride (SOCl2, Avra), nitric acid (HNO3, Rankem), tetrahydrofuran (THF, Rankem), cobalt nitrate (Co(NO₃)₂, (Nice Chemicals) N, N'-dimethyl formamide (DMF, Avra), sodium hydroxide (NaOH, Qualigens Fine chemicals), potassium hydroxide (KOH, Nice) ptoluene sulfonic acid (p-TSA, Avra), ethanol (Rankem), selenium dioxide (SeO2, Nice) were used as such. The Screen-printed carbon working electrode (SPCE) (0.07cm²) received from Zensor R&D Co. Ltd, Taiwan. The morphology and microstructure of Co₃O₄@Se NPs/MWCNTs nanocomposite was analyzed using a scanning electron microscope (SEM; Jeol JSM 6390, USA) and an X-ray diffractometer (PANalytical/ XPert3 Powder, UK), respectively. The Co₃O₄@Se NPs/MWCNTs nanocomposite was also characterized using a Fourier transform infrared (FTIR) spectrophotometer (Perkin Elmer Model: Spectrum Two, USA) and UV-Visible spectrophotometer (INTECH 294, India). The electrochemical performances were recorded at room temperature with a programmed electrochemical work station (OrigaLys-OFG500, France).

2.2. Synthesis of Co₃O₄@Se NPs/MWCNTs nanocomposite

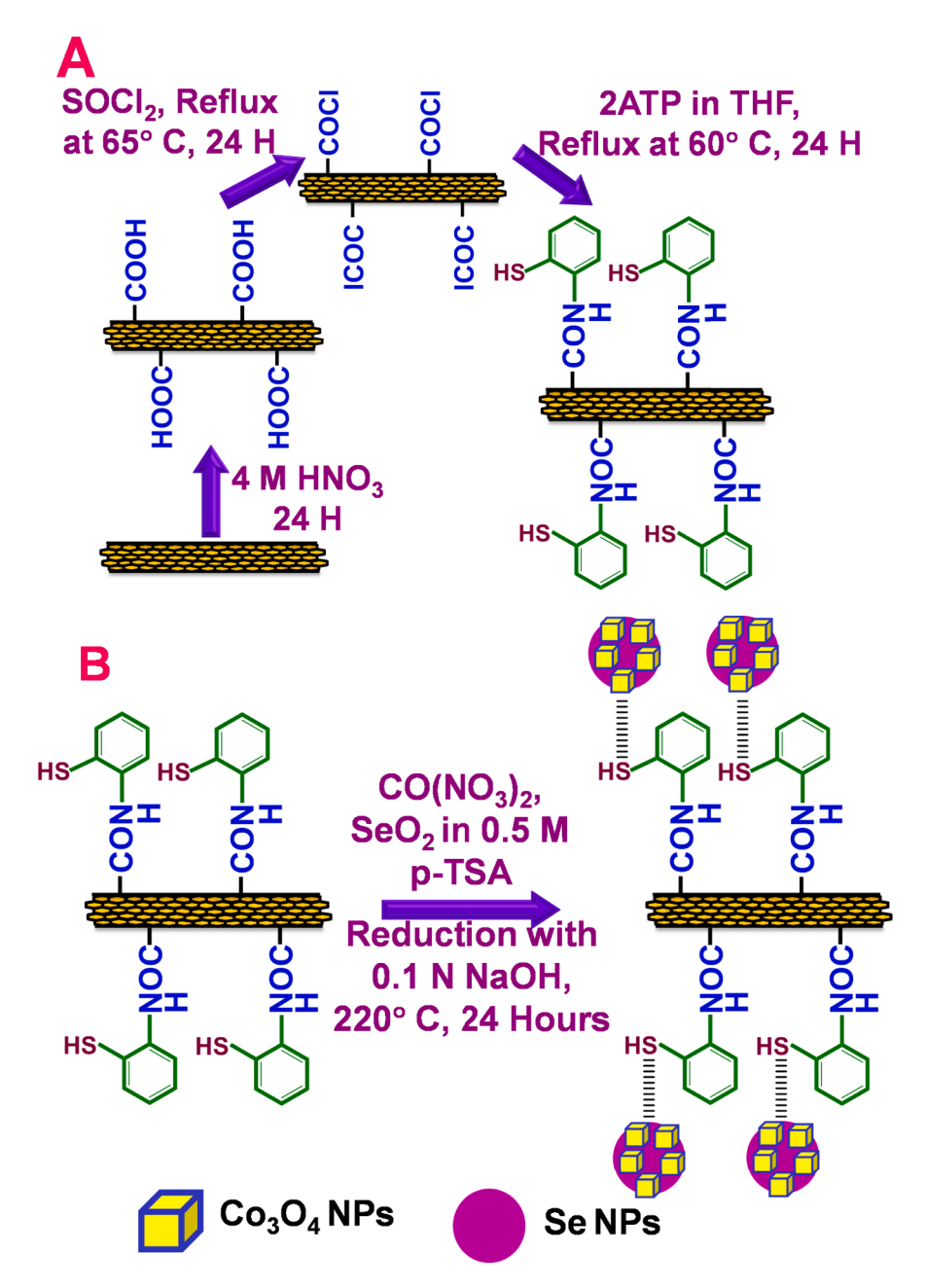
MWCNT was thiol functionalized using 2-aminothiophenol as reported earlier [27]. The synthesis of Co_3O_4 @Se NPs/ MWCNTs nanocomposite was carried out using a simple hydrothermal method. The schematic procedure for the preparation of MWCNTs and Co_3O_4 @Se NPs/MWCNTs nanocomposite are illustrated in the Scheme 1. The Co_3O_4 @Se NPs/MWCNTs nanocomposite was synthesized by mixing an appropriate amount of MWCNTs (0.1 g), $\text{Co}(\text{NO}_3)_2$ (0.25 g) and SeO₂ (0.5 g) in 70 mL aqueous solution of p-TSA (0.5 M) under ultrasonication for about 30 min. Then 0.1 N NaOH (2.0 mL) was added in drops and the solution was stirred for 30 mins. After stirring, the solution was transferred to a 100 mL Teflon autoclave and heated to 220°C for 12 h The resulting black precipitate of Co_3O_4 @Se NPs/MWCNTs nanocomposite was centrifuged, washed several times with distilled water and dried at 50 °C for 12 h in hot air oven.

2.3. Fabrication of MWCNTs & Co₃O₄@Se NPs/MWCNTs modified electrode and its electrochemical studies

The ${\rm Co_3O_4@Se}$ NPs/MWCNTs modified electrode was fabricated by drop casting method by DMF on screen printed carbon electrode (SPCE). For comparison, the modified MWCNTs nanocomposite electrode also fabricated with the same procedure. Electrochemical analysis is accomplished to examine the capacitive behavior of prepared samples. All electrochemical measurements were carried out in a conventional three-electrode electrochemical system using (OrigaLys-OFG500, France). Modified Screen printed carbon electrode (SPCE) was used as a working electrode while Platinum wire and Ag/AgCl electrode were utilized as counter and reference electrode respectively, to establish their electrochemical and capacitance parameters at room temperature. 1 M KOH was used as electrolyte solution for electrochemical analysis. The specific capacitance values were calculated from CV by integrating the electroactive area and also using charge–discharge curves.

2.4. Antimicrobial activity of $Co_3O_4@Se\ NPs/MWCNTs$ nanocomposite

Kirby Bauer Agar well diffusion method was employed to study the antimicrobial efficacy of Co_3O_4 @Se NPs/MWCNTs nanocomposite against gram-negative (G-) bacteria (Escherichia coli (E. coli, MTCC-739) and Pseudomonas aeruginosa (P. Aeruginosa, MTCC-1688)) and fungus (Candida albicans (C. Albicans, MTCC-227)). Clinical isolates of cultures were obtained from Microbial Type Culture Collection and



 $\textbf{Scheme 1.} \ \, \textbf{(A) Functionalization of MWCNT and (B) Preparation of Co}_3O_4 @Se \ NPs/MWCNTs \ nanocomposite.$

Gene Bank (MTCC), CSIR Institute of Microbial Technology, Chandigarh, India and the strains were preserved on Nutrient agar slants at 4 $^{\circ}\text{C}$. Gentamicin (10µg /disk) and DMF (100µl) were used as positive and negative control, respectively. The three clinical isolates were grown in nutrient broth at 37°C for 8 h The nutrient agar medium pre-sterilized by autoclaving for 15 min at 121°C (15 Ibs pressure) was transferred into sterilized petri plates and allowed to solidify. Subsequently, the agar wells were prepared using well cutter. The Co₃O₄@Se NPs/MWCNTs nanocomposite stock solution was prepared in DMF at the concentration of 1 mg/1 mL. Then, the wells were loaded with different volumes (25, 50, 75 and 100µl) of DMF dissolved solution of Co₃O₄@Se NPs/MWCNTs nanocomposite. The petri plates were incubated at 37°C for 24 h The antimicrobial activity of Co₃O₄@Se NPs/MWCNTs nanocomposite was evaluated by zone of inhibition (expressed in millimeter). For comparison, the microbicidal effect of MWCNTs was also tested.

3. Results and discussion

3.1. Morphology and microstructure of Co₃O₄@Se NPs/MWCNTs nanocomposite

The surface morphology of the prepared samples was characterized by scanning electron microscopy (SEM). SEM was recorded to investigate the surface modification of pristine MWCNTs by thiol (–SH) functionalization and presence of $\rm Co_3O_4@Se$ NPs onto MWCNTs. Fig. 1 displays the SEM images of MWCNTs (Fig. 1a) and $\rm Co_3O_4@Se$ NPs/MWNTs nanocomposite (Fig. 1b). The SEM image of MWCNTs exhibited uniformly distributed bright white spots with debundled tubes. It demonstrates that the nanotubes become more active at the ends/sidewalls due to functionalization of pristine MWCNTs [45]. From the image of $\rm Co_3O_4@Se$ NPs/MWCNTs nanocomposite (Fig. 1b), it is presumed that the nanospherical-shaped Se NPs of size \sim 50 nm are distributed on the surface of MWCNTs. It is due to the exceptional anchoring ability of thiol

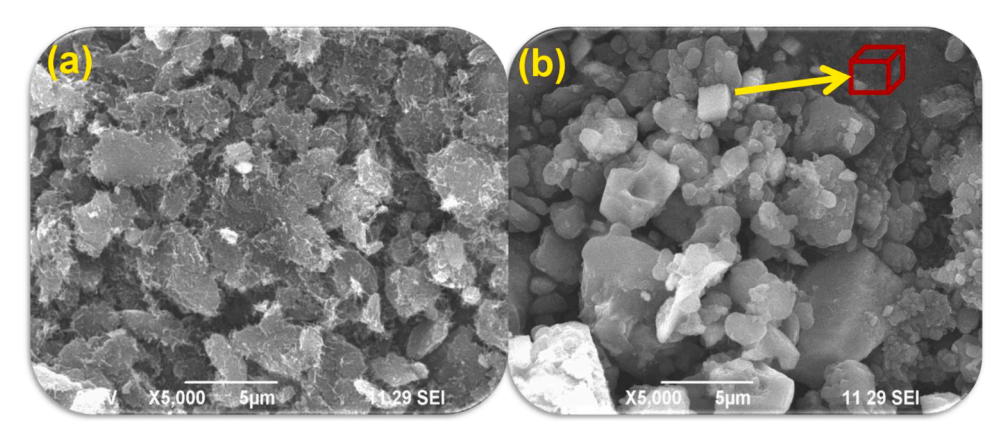


Fig. 1. SEM image of (a) MWNTs and (b) Co₃O₄@Se NPs/MWNTs nanocomposite.

(-SH) groups present on MWCNTs to metal/metal oxide nanoparticles [28]. The incorporation of thiol (-SH) group augments the surface activity of the MWCNTs leading to high binding ability towards Se NPs [46]. Besides, it has been witnessed that the surface of MWCNTs is covered completely with nanocube-shaped Co₃O₄ NPs of size ~ 300 nm. Se NPs exhibits advantageous physicochemical properties like high particle dispersion, good adsorption ability and more active surface area [47]. We envisage that Se NPs with beneficial properties offer a good coordination sites to Co₃O₄ NPs which resulted in good distribution and loading of Co₃O₄ NPs on the surface of Se NPs.Hence, more numbers of nanocube-shaped Co₃O₄ NPs are anchored on the surface of Se NPs through physical adsorption mechanism. It is clearly acknowledged from the SEM image of Co₃O₄@Se NPs/MWCNTs nanocomposite (Fig. 1b) that the nanospherical-shaped Se NPs are wrapped by nanocube-shaped Co₃O₄ NPs. However, the shortcomings of Se NPs such as enlargement and aggregation into large clusters in aqueous medium are leading to a poor performance/activity and further affect its applications. Hence, a suitable substrate is essential to avoid such problems associated with Se NPs [48]. In this present work, we have taken care in avoiding aggregation of Se NPs by using MWCNTs as substrate. The interaction of -SH groups in MWCNTs with Se NPs enhances uniform distribution, surface enrichment and stability of Se NPs against aggregation/leaching processes [49]. The unique features of thiol (-SH) groups are exploited to adsorb and disperse Co3O4@Se NPs throughout the entire surface of MWCNTs.

The crystallinity and phase characteristics of as-synthesized samples were surveyed by X-ray diffraction (XRD) analysis. As can be seen in Fig. 2a that the diffraction peaks located at $2\theta = 26.0^{\circ}$, 43.1° and 53.7° correspond to the (002), (100) and (004) reflection planes of MWCNTs [50]. Fig. 2b depicts the XRD pattern of $Co_3O_4@Se$ NPs/MWCNTs

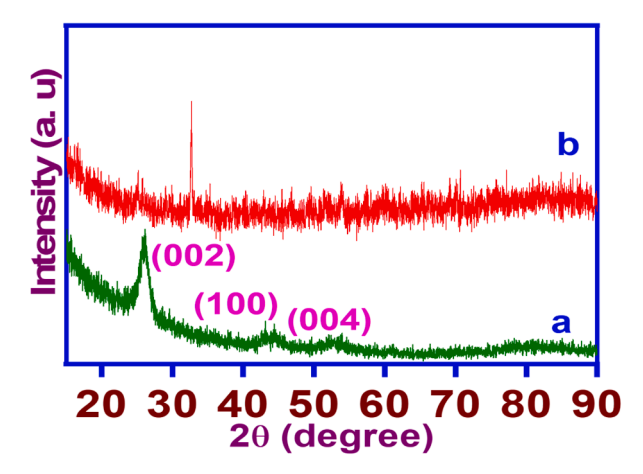


Fig. 2. XRD of (a) MWCNTs and (b) Co₃O₄@Se NPs/MWCNTs nanocomposite.

nanocomposite. It exhibited the signature diffraction peaks of Co3O4 nanoparticles at $2\theta = 18.86^{\circ}$, 32.69° , 36.94° , 38.55° , 44.89° , 55.89° , 59.43°, and 65.27° which are assigned to the (111), (220), (311), (222), (400), (422), (511), and (440) lattice planes, respectively. All these peaks are well indexed with the cubic phase of Co₃O₄ nanoparticles [51–53]. Besides, Co₃O₄@Se NPs/MWCNTs nanocomposite possessed diffraction peaks at $2\theta = 24.1^{\circ}$, 29.90° , 41.37° , 43.75° , 45.41° , 47.23° , 51.42°, 55.90°, 61.40°, 65.22° and 71.12° which are attributed to the (100), (101), (110), (102), (111), (200), (201), (112), (202), (210) and (113) lattice planes, respectively, of a hexagonal phase of Se NPs [49]. The following observations are arrived from the XRD peak intensities of Co₃O₄@Se NPs/MWCNTs nanocomposite: (i) The average particle size was calculated using Debye Scherrer formula for Se NPs 29.90° (101) plane) and Co_3O_4NPs (32.69° (220) plane). It was estimated that ~ 40 nm and ~ 300 nm for Se NPs and Co₃O₄ NPs, respectively, which corroborates with the average particle size observed through SEM analysis (Fig. 1b), (ii) Since, Se NPs exhibited exceptional properties as mentioned in SEM analysis, more amounts of larger Co₃O₄ NPs are anchored on the entire available surface area of smaller Se NPs. Hence, Se NPs shows less intense peaks compared to Co₃O₄ NPs, (iii) The sharp and well defined diffraction peaks for Se NPs as well as Co₃O₄ NPs reveals their crystalline nature, (iv) The presence of less intense signature peaks of MWCNTs are ascribed to the complete surface coverage of MWCNTs by Co₃O₄@Se NPs [54] (v) The appearance of characteristic peaks of MWCNTs in nanocomposites ensures that the surface of MWCNTs is not affected even after the adsorption of Co₃O₄@Se NPs onto MWCNTs and (vi) The characteristic peak intensities of MWCNTs in Co₃O₄@Se NPs/MWCNTs nanocomposite (Fig. 2b) are subdued which is due to the introduction of Co₃O₄@Se NPs onto MWCNTs. The aforementioned observations confirmed that the material is a nanocomposite of MWCNTs and Co₃O₄@Se NPs.

3.2. Spectral behaviour of Co₃O₄@Se NPs/MWCNTs nanocomposite

FTIR analysis has been carried out to obtain further insight into the nanocomposite formation and successful preparation of MWCNTs. Fig. 3 represents the FTIR spectrum of MWCNTs (Fig. 3a) and Co₃O₄@Se NPs/ MWCNTs nanocomposite (Fig. 3b). In Fig. 3a, the presence of peak at 3426 cm $^{-1}$ is assigned to stretching vibration of N–H in 2ATP [37]. The band observed around 1637 cm $^{-1}$ which corresponds to the stretching vibration of carbonyl bond (C = O) of amide group [22].The peak located at 1406 cm $^{-1}$ is due to the stretching vibration of C—N-C bond which could confirm the occurrence of amidation reaction between the amine (–NH₂) group of 2ATP and the COCl groups onto MWCNTs [42]. The FTIR spectrum of MWCNTs exhibits a peak at 1558 cm $^{-1}$ is assigned to C = C stretching vibrations of benzenoid rings in 2ATP [43,55-57]. The absorption peaks at 2351 cm $^{-1}$ and 620 cm $^{-1}$ which are due to the stretching vibration of S–H [23] and C–S [34] bond, respectively. Hence,

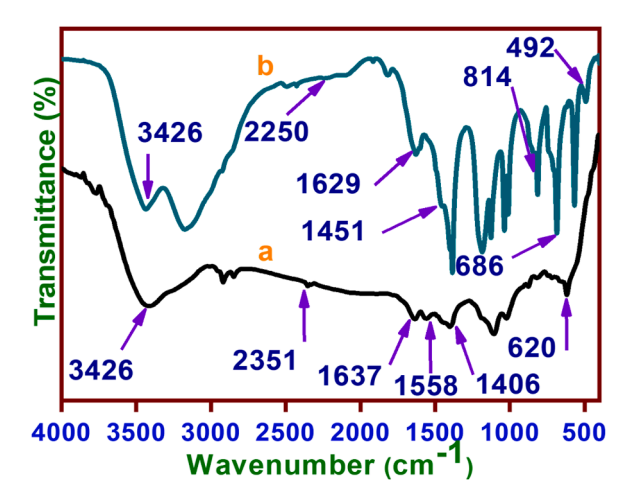


Fig. 3. FTIR spectrum of (a) MWCNTs and (b) ${\rm Co_3O_4@Se}$ NPs/MWCNTs nanocomposite.

the characteristic FTIR spectral peaks of MWCNTs authenticates the successful covalent functionalization of MWCNTs surface with 2ATP.

In order to probe the genuine preparation of Co₃O₄@Se NPs/ MWCNTs nanocomposite, FTIR was recorded and the result is presented (Fig. 3b). The effective formation of Co₃O₄@Se NPs/MWCNTs nanocomposite is established by monitoring the following changes in the peak/band intensity/position of nanocomposite: (i) The slight shifts in the position of the characteristic peaks/bands of MWCNTs after incorporation of Co₃O₄@Se NPs onto MWCNTs suggests that there can be a molecular level interaction between Co₃O₄@Se NPs and MWCNTs [58] (ii) The appearance of new vibration absorption peak at 1451 cm⁻¹ with concomitant disappearance of peak for benzenoid ring is related to C = C stretching vibrations of the quinoid ring in 2ATP [59]. This may be presumably due to the fact that the incorporation of Co₃O₄@Se NPs on to MWCNTs induces the electron movement through aromatic ring of 2ATP. Hence, it results in generation of more conductive quinoid units [44], (iii) On close analysis, the vibration peak corresponds to S-H group is vanished in the FTIR spectrum of Co₃O₄@Se NPs/MWCNTs nanocomposite (Fig. 3b). Binding of Co₃O₄@Se NPs onto MWCNTs surface could restrict the vibration of thiol (-SH) groups. It makes certain the loading of Co₃O₄@Se NPs onto MWCNTs [50] (iv) A new less intense peak emerged at 2250 cm⁻¹ indicates the formation of Se NPs [46], (v) The absorption peak located at 686 cm⁻¹ is related to the Co-O stretching vibration [47], (vi) The presence of intense absorption peak at 814 cm $^{-1}$ corresponds to Se-O stretching vibration [48]. It supports the physisorption of Co₃O₄ NPs on the surface of Se NPs through its oxygen atoms. The advantageous properties of Se NPs promote effectual adsorption of more amounts of Co₃O₄ NPs onto Se NPs, (vii) Low intense peak observed at 492 cm⁻¹ is ascribed to the vibration of Se–S [49]. The adsorbed Co₃O₄ NPs onto Se NPs suppresses the stretching vibration of Se-S bond and (viii) The appearance of less intense peak for Se NPs

(2250 cm $^{-1}$) and intense peaks for Co-O stretching vibration (686 cm $^{-1}$)/Se–O stretching vibration (814 cm $^{-1}$) suggests that anchoring of large numbers of Co₃O₄ NPs onto Se NPs through physical adsorption process could restrict the vibration of Se NPs. The above-mentioned spectral characteristics validate the formation of a nanocomposite comprising of MWCNTs and Co₃O₄@Se NPs.

In order to establish further the synthesis of Co₃O₄@Se NPs/ MWCNTs nanocomposite, UV-Visible spectroscopy is used to probe the interactions between MWCNTs and Co₃O₄@Se NPs. For this, UV-Visible spectrum of MWCNTs and Co₃O₄@Se NPs/MWCNTs nanocomposite were recorded and displayed (Fig. 4A). The UV-Visible spectrum of the MWCNTs exhibits a strong absorption peak at 270 nm which is assigned to π - π * of aromatic C = C bonds of MWCNTs [50,60-62]. The formation of Co₃O₄@Se NPs/MWCNTs nanocomposite is authenticated from the following observations: (i) Spherical shaped Se NPs in the nanocomposite display its typical plasmonic resonance band as a small hump around 550 nm [54], (ii) A small shoulder observed around 273 nm is attributed to the presence of Co₃O₄ nanoparticles in the nanocomposite [58], (iii) The appearance of less intense hump for Se NPs is presumed that the entire surface of Se NPs because of its beneficial inherent properties is completely covered with Co₃O₄ NPs, and (iv) After the incorporation of Co₃O₄@Se NPs onto MWCNTs, the signature peak of MWCNTs is subdued with blue shift to 268 nm. It indicates the existence of a strong molecular level interaction between MWCNTs and Co₃O₄@Se

Besides, the band gap value was calculated by Tauc method using the absorbance values (From UV-Visible spectral data). It suggests that the optical absorption strength depends on the difference between the photon energy and the bandgap. The optical band gap (Eg) can be estimated by the Tauc's relation i.e., $(\alpha h \upsilon)^{1/n} = A(h \upsilon - E_g)$, where α is the absorption coefficient, $h\nu$ is the photon energy, A is a constant that depends on the transition probability and the factor n represents nature of the transition which theoretically equal to 2 and 1/2 for allowed indirect and direct electronic transition, respectively. The plot $(\alpha h \upsilon)^{1/n}$ vs $h\upsilon$ at a given n value shows the transition type and the interception point with the x axis (energy axis) provides the direct energy band-gap value. Fig. 4B depicts the Tauc plot of MWCNTs and Co₃O₄@Se NPs/MWCNTs nanocomposite at n = 2. The direct band gap value of Co_3O_4 @Se NPs/ MWCNTs nanocomposite (4.17 eV) is higher than that of MWCNTs (3.86 eV). The band gap of MWCNTs was increased after the incorporation of Co₃O₄@Se NPs into the MWCNTs matrix. It is presumed that there is an electronic transition between MWCNTs matrix and Co₃O₄@Se NPs.

3.3. Electrochemical performance evaluation

3.3.1. Cyclic voltammetry (CV) behavior of the modified SPCE/MWCNTs & SPCE/Co₃O₄@Se NPs/MWCNTs nanocomposite

The cyclic voltammetric (CV) curves of the modified MWCNTs & Co_3O_4 @Se NPs/MWCNTs nanocomposite on SPCE in 1 M KOH aqueous electrolyte are shown in Fig. 5(A). Fig. 5(A) illustrates the cyclic

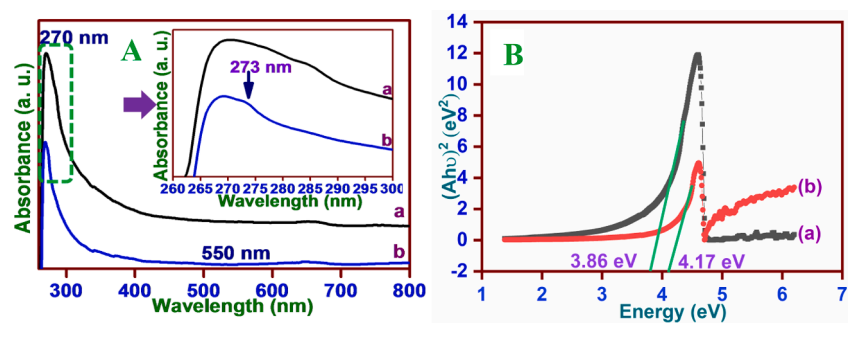


Fig. 4. (A) UV-Visible spectrum and (B) Tauc plot of (a) MWCNTs and (b) Co₃O₄@Se NPs/MWCNTs nanocomposite.

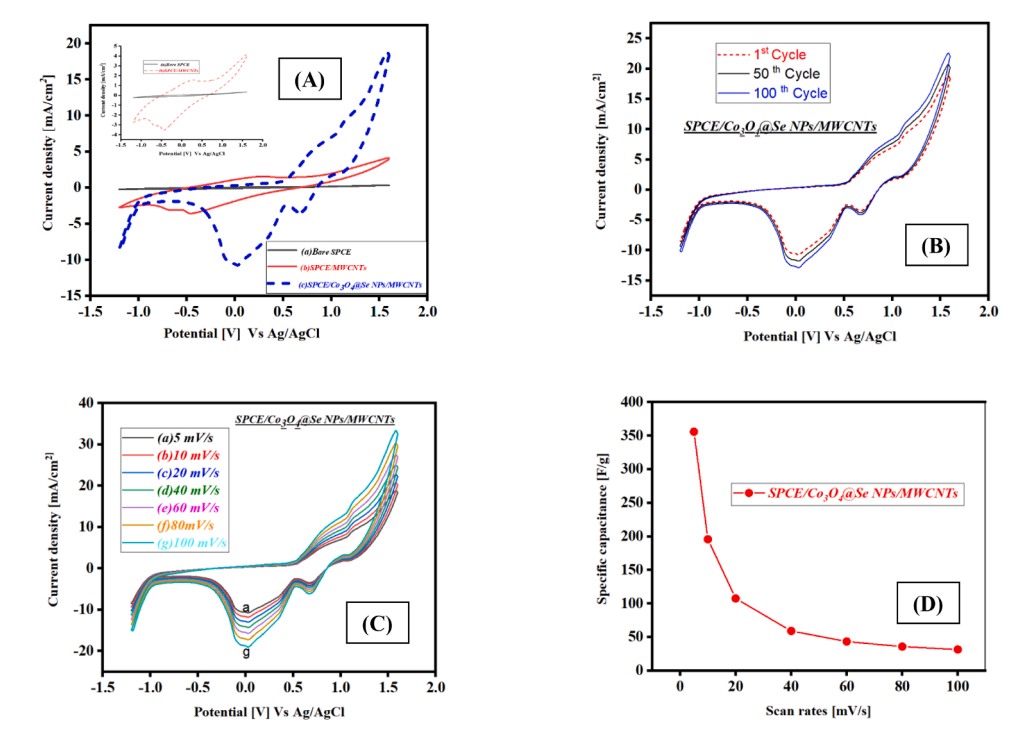


Fig. 5. (A). Cv peaks of (a) Bare SPCE (b) SPCE/MWCNTs and (c) SPCE/Co₃O₄@Se NPs/MWCNTs nanocomposite (B) Stability of SPCE/Co₃O₄@Se NPs/MWCNTs (C) SPCE/Co₃O₄@Se NPs/MWCNTs at various scan rates and (D) Scan rates Vs Specific capacitance of SPCE/Co₃O₄@Se NPs/MWCNTs nanocomposite.

voltammetric performance of (a) Bare SPCE (b) SPCE/MWCNTs & (c) SPCE/Co₃O₄@Se NPs/MWCNTs nanocomposite electrode with the potential window between -1.2 and 1.6 V at a scan rate of 5 mV/s. The electrochemical potential windows are adjusted according to the locations of the redox couples. A pair of redox patterns are observed around 0.13, 0.8 V with its counter parts nearby 0.03, 0.6 V (Vs Ag/AgCl) respectively. These electrochemical signatures with increased current density pattern were observed from Fig. 5A (c) indicates the electroactive interactions amid SPCE/Co₃O₄@Se NPs/MWCNTs nanocomposites and reversible transitions of Co₃O₄ and CoOOH (II/III) and between CoOOH and CoO₂ (III/IV). The reactions are represented below (i &ii): [59,63],

$$Co_3O_4 + OH - + H_2O \leftrightarrow 3CoOOH + e -$$
 (i)

$$CoOOH + OH - \leftrightarrow CoO_2 + H_2O + e -$$
 (ii)

There are no significant peaks are shown in the CV pattern for bare SPCE in (Fig. 5A (a)). Fig. 5A (b) detailed CV pattern, there is a slight pair of redox peaks were witnessed for SPCE/MWCNTs. In comparison, the presence of SPCE/Co₃O₄@Se NPs/MWCNTs nanocomposite escalated the higher current density than the other modified electrodes. The properties of thiol (–SH) groups have been properly exploited in effective anchoring and distribution of Co₃O₄@Se NPs grafted onto MWCNTs. This effective interaction augments superior electron transfer kinetics pathways between the constituents. Thus, due to the improved current density with superior electron transfer characteristics of the SPCE/Co₃O₄@Se NPs/MWCNTs nanocomposite electrode was chosen for further electrochemical investigations.

The SPCE/Co₃O₄@Se NPs/MWCNTs nanocomposite electrocatalytic material have an excellent significance over the stability factor. The recorded CV pattern till 100th cycle ensures the stability of the synthesized modified nanocomposite electrode (SPCE/Co₃O₄@Se NPs/MWCNTs) (Fig. 5B). The stability cycling pattern illustrates comparison of the 1st cycle, 50th and the 100th cycle, a slight variation in the current density was noticed but there is no obvious declination occurs in the reaction. Thus SPCE/Co₃O₄@Se NPs/MWCNTs demonstrates the steadiness of composited materials.

CV peaks at different scan rates from 5 to 100 mV/s (i.e. 5,20,40,60,80,100 mV/s) in the potential series of -1.2 to 1.6 V is revealed in Fig. 5C. The CV peaks retain their original shape even at high scan rate (100 mV/s) with raising current density signifying good electrochemical reversibility desirable for high power supercapacitor. The current under CV curve gradually increased with scan rate. This reveals that the voltammetric current is directly proportional to the scan rates of CV, representing an ideally capacitive behavior. The specific capacitance of the SPCE/Co₃O₄@Se NPs/MWCNTs measured graphically by integrating the electroactive surface area in the CV peak using the following Eq. (1) [4,6,59,63,64].

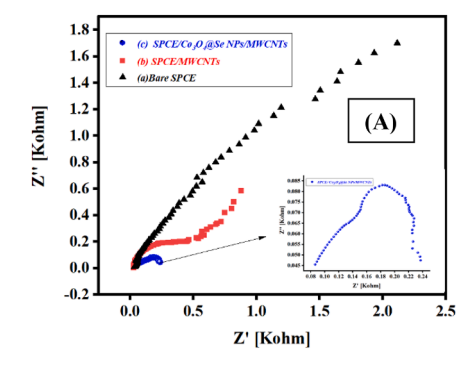
$$Csp = \int Idv / m * s * dv \tag{1}$$

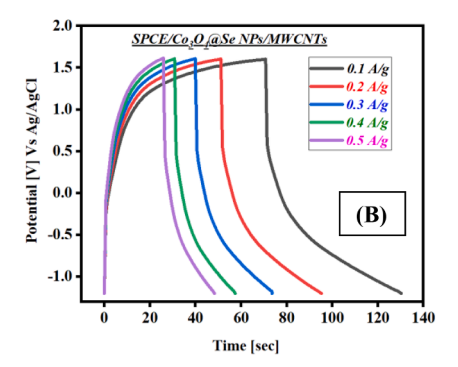
where m is the mass of the electroactive material (g) of the electrode sample and s is the scan rate (mV/s) and dv is change in voltage (V).

The maximum specific capacitance was estimated at 5 mV/s was 356 F/g. The specific capacitance values start to fall from 356 to 31.5 F/g by increasing the scan rate as depicted in Fig. 5D (specific capacitance Vs Scan rate). This was generally due to the transfer rate of ions becomes slower with increasing scan rate which tend to either depletion or saturation of protons in the electrolytes inside the electrode during the re-dox process. This outcome in an increase in ionic resistivity which leads to a drop in the capacitance of the electrode. Thus, the excellent electrocatalytic, better stability and supercapacitive performances of SPCE/Co₃O₄@Se NPs/MWCNTs originated from the synergistic effect of them [64,65]. So, this type of composites can be reflected as promising materials for supercapacitor applications.

3.3.2. Electrochemical impedance spectroscopy (EIS) study

Fig. 6A (inset displays the magnified EIS plot) shows the electrochemical impedance spectrum (Nyquist plot) of (a) Bare SPCE (b) SPCE/MWCNTs and (c) SPCE/Co₃O₄@Se NPs/MWCNTs nanocomposite electrode. In the high frequency region, a semi-circle with low charge transfer resistance (Rct) confirms the SPCE/Co₃O₄@Se NPs/MWCNTs ($\sim 0.16~\rm K\Omega)$ modified electrode owns high electrical conductivity than





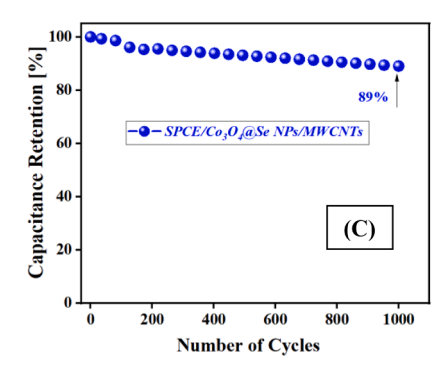


Fig. 6. (A). EIS spectra of (a) Bare SPCE (b) SPCE/MWCNTs and (c) SPCE/ Co_3O_4 @Se NPs/MWCNT nanocomposite (B) GCD curve of SPCE/ Co_3O_4 @Se NPs/MWCNT nanocomposite and (C) Capacity retention of SPCE/ Co_3O_4 @Se NPs/MWCNT nanocomposite electrode.

SPCE/MWCNTs ($\sim0.4~\text{K}\Omega$ and Bare SPCE $\sim0.5~\text{K}\Omega$). This elucidation point outs a low charge transfer resistance in the electrochemical system and a prominent capacitive performance [66]. The electrical conductivity of the nanocomposite electrode elevated due to the fusion and the synergistic interaction between the materials. The attained EIS plot ensured the ease of electron transfer pathway for SPCE/Co $_3$ O $_4$ @-SeNPs/MWCNTs nanocomposite electrode which coincides with the CV outcomes.

3.3.3. Electrochemical properties of fabricated SPCE/Co3O4@Se NPs/ MWCNTs modified electrode towards supercapacitance performances by GCD technique

In Fig. 6B GCD curves represents the charge–discharge behavior of the SPCE/Co $_3$ O $_4$ @Se NPs/MWCNTs modified electrode within the fixed potential width of -1.2 V to 1.6 V with various current densities (0.1 to 0.5 A/g) in presence of 1 M KOH. It is inferred that the achieved charge curves are moreover same to the discharging curve, but there is an insignificant difference in the charging as well as discharging time. Also, during the discharge-charge cycle a low voltage drop was observed and it specifies the improved conductivity of the materials. The average specific capacitance of the synthesized nanocomposite electrode ($\sim\!212$ F/g) was estimated from the Eq. (2) using charge–discharge curves [4, 6].

$$Cm = Id. \Delta t d/m.\Delta V$$
 (2)

Here, Id -discharging current (A), Δtd -discharging time (sec), ΔV -change in voltage (V), and m-the electro-active mass (g) on the modified SPCE electrode substrate.

Also, the coulombic efficiency of the SPCE/ Co_3O_4 @Se NPs/MWCNTs modified electrode is about 84% was assessed using Eq. (3).

Coulombic efficiency
$$\% = (\Delta td / \Delta tc) * 100\%$$
 (3)

Here, Δtc (sec) and Δtd (sec) are change in charging and discharging time.

The capacitor discloses the superior cycling retention of 89% after 1000 cycles (Fig. 6C). There is a slight early irregular deviation in Csp at

95% is owing to the slightly dispersion of SPCE/Co $_3$ O $_4$ @Se NPs/MWCNTs into the electrolyte while it is immersed for an instant, later it was found stabilized and an estimable reversibility with an 89% was attained. The occurred results designate that superior electrode cycling stability due to the synergistic interaction amid the constituents as well as the functionalized thiol (–SH) group influences in the enrichment of Co $_3$ O $_4$ @Se NPs onto MWCNTs.

3.4. Antimicrobial activity

The antimicrobial activity of MWCMTs and Co_3O_4 @Se NPs/MWCNTs nanocomposite was tested against gram-negative (G-) bacteria (E. coli and P. aeruginosa) and fungus (C. albicans) as model micro-organisms[50]. The antimicrobial activity has been measured by standard zone of Inhibition (ZOI) microbiology assay. Fig. 7 demonstrates the antimicrobial activity result of MWCMTs (Fig. 7a) and Co_3O_4 @Se NPs/MWCNTs nanocomposite (Fig. 7b) on various pathogens. The inhibition zone (mm) values against pathogens for both MWCMTs and Co_3O_4 @Se NPs/MWCNTs nanocomposite are listed in Table 1. Gentamicin was used as a standard to evaluate the efficacy of antimicrobial activity with MWCMTs and Co_3O_4 @Se NPs/MWCNTs nanocomposite. From the zone of inhibition values, it is observed that the Co_3O_4 @Se NPs/MWCNTs nanocomposite exhibited potent microbicidal effect on pathogens than MWCNTs (Table 1).

Generally, the physical properties such size, surface area, polar surface, morphology, adsorption etc. enhances the antimicrobial efficacy of nanoparticles [67–70]. The antibacterial activity of Co_3O_4 @Se NPs/MWCNTs nanocomposite is due to the existence of electrostatic, hydrophobic, van der Waals or receptor-ligand interactions between negatively charged bacterial cells and positively charged Co_3O_4 NPs [58, 71,72]. Since G- bacterial cell surface carrying more negative charges from lipopolysaccharides, the positively charged Co^{2+} can attach with negatively charged cell membrane through these interactions [54]. Hence, it is revealed vivid that the binding of Co^{2+} with negatively charged surface of G- bacteria through electrostatic interaction facilitated the induction of reactive oxygen species (ROS) and hydroxyl free

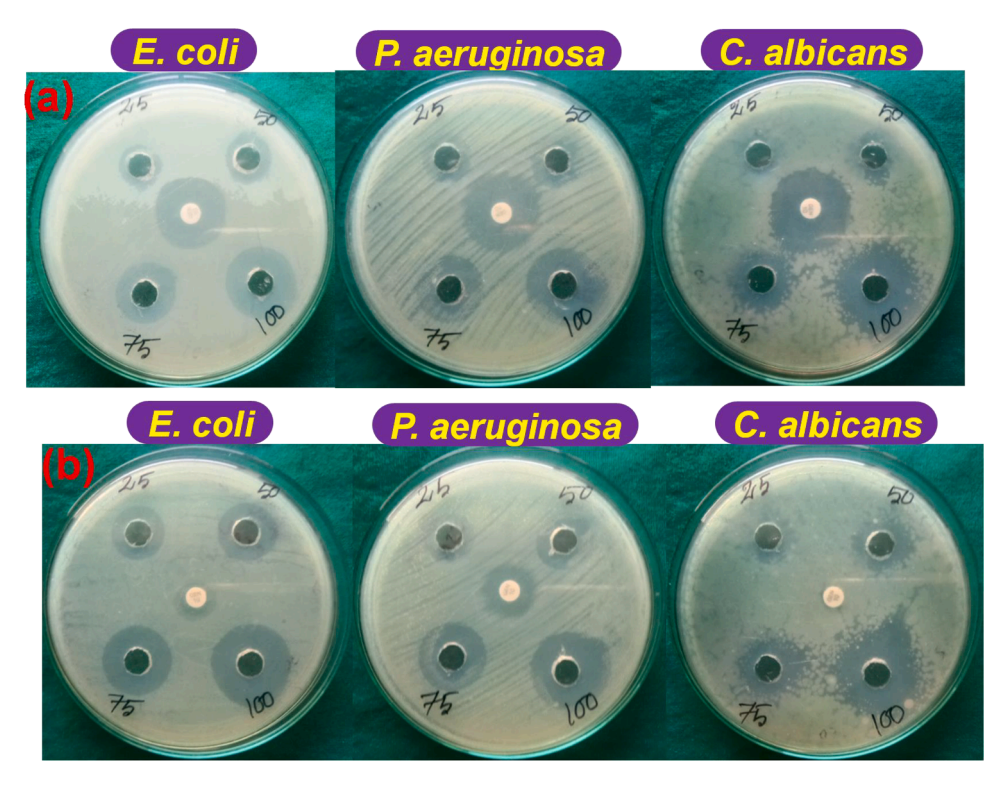


Fig. 7. Antimicrobial activity of (a) MWCNTs and (b) Co₃O₄@Se NPs/MWCNTs nanocomposite against various pathogens.

Table 1Antimicrobial effect of synthesized samples against various pathogens.

	,		U			U	
Samples	Pathogen	inhib 25	ition (n 50	nm/ml) 75	100	d Zone of Reference Antibiotic ^a	
		μl	μl	μl	μl	Allubiotic	
MWCNTs	E. coli	12	15	18	22	32	
	Pseudomonas aeruginosa	14	17	20	22	34	
	Candida albicans	14	12	24	25	34	
Co ₃ O ₄ @Se	E. coli	18	20	20	25	32	
NPs/ MWCNTs	Pseudomonas aeruginosa	16	19	22	27	34	
	Candida albicans	18	20	22	28	34	

 $^{^{\}rm a}$ Gentamic in (10 $\mu g/disc)$ antibiotic as standard antibiotics for all the pathogens.

radicals, which could cause cell death [27,73]. Besides, it is pertinent to note that ${\rm Co_3O_4@Se}$ NPs/MWCNTs nanocomposite exhibited a significant antifungal activity with the zone of inhibition of 28 mm against fungi (C. albicans) as compared to positive control, Gentamicin (22 mm).

Since, Se NPs possesses very vital and mandatory properties such as high particle dispersion, high adsorption, morphology and large surface area, it has been considered as a promising antimicrobial agent [13]. As a negative, usually Se NPs are highly unstable in aqueous media and are apt to aggregate into bulk. These tendencies result in loss of activities of Se NPs [24,74]. Hence, it is essential to choose a suitable substrate/stabilizing agent to enhance good stability and dispersion of Se NPs in aqueous medium. For this purpose, in this present investigation, MWCNTs has been preferred as a disperser and stabilizer to Se NPs. The most advantageous features of thiol (–SH) group in MWCNTs were exploited to anchor more numbers of Se NPs onto MWCNTs. As a result, Se NPs with inbuilt meritorious properties could augment physisorption of more amounts of Co_3O_4 NPs on its surface. The intertwined

performance of both Co_3O_4 NPs and Se NPs was used to study the microbicidal efficiency of Co_3O_4 @Se NPs/MWCNTs nanocomposite towards various pathogens.

The probable reasons for antimicrobial activity of MWCNTs are given here: (i) Debundled nature of MWCNTs is due to effective functionalization of MWCNTs with 2ATP. It may enhance the antimicrobial action of MWCNTs [67],(ii) The higher dispersibility of MWCNTs due to thiol (-SH) functionalization may promote its antimicrobial activity [26] (iii) MWCNTs provide concomitant capture and deactivation of micro-organism through microbial sorption [67] (iv) The electron-donating nature of thiol (-SH) group present in 2ATP triggers the jumping of electrons through the benzene ring of 2ATP. It results in the formation of positively charged thiol (-SH) sites in 2ATP. Thus, there may be a chance for adsorption of positively charged thiol (-SH) group onto the negatively-charged cell membrane [63], (v) Covalent functionalization of surface of MWCNT with higher stability and lesser toxicity can promote /augment the antimicrobial activity of MWCNTs [75,47], (vi) The hydrogen bond formation between the thiol (-SH) groups of MWCNTs and hydroxyl (-OH) groups of cell membrane of microbes which can inhibit the growth of the cells and (vii) Attachment of MWCNTs on the cell membrane surface [76]. The advantageous properties of thiol (-SH) groups could facilitate significantly superior antimicrobial activity of Co₃O₄@Se NPs/MWCNTs nanocomposite against micro-organisms.

4. Conclusions

The present work demonstrates a facile hydrothermal strategy to synthesize a nanocomposite (Co_3O_4 @Se NPs/MWCNTs) comprising of thiol (–SH) functionalized multiwalled carbon nanotube (MWCNTs) and cobalt oxide adsorbed onto selenium nanoparticles (Co_3O_4 @Se NPs). The marginal shift in position with change in intensity of signature peak/band of MWCNTs observed in microstructural and optical studies after the incorporation of Co_3O_4 @Se NPs clearly envisaged that there must be a molecular level interaction between MWCNTs and Co_3O_4 @Se NPs. Besides, the XRD, FTIR and UV–Visible analysis of Co_3O_4 @Se NPs/

MWCNTs nanocomposite revealed the existence of Co₃O₄ NPs and Se NPs on the surface of MWCNTs. All these features acknowledged the genuine formation of nanocomposite consisting of Co₃O₄@Se NPs and MWCNTs. Co₃O₄@Se NPs/MWCNTs nanocomposite exhibits supercapacitive performances and microbicidal activity against Gramnegative (G-) bacteria (E. coli and Pseudomonas aeruginosa) and fungus (Candida albicans). It showed excellent specific capacitance 356 F/g with good cyclic stability and superior inhibitory effect towards the growth of pathogens. The presence of thiol (-SH) group onto MWCNTs plays a very crucial role in enhancing the electrochemical performance as well as antimicrobial activity of Co₃O₄@Se NPs/MWCNTs nanocomposite. The influence of beneficial properties of thiol (-SH) functionalized group was used in stabilizing and distributing (without aggregation) Co₃O₄@Se NPs onto MWCNTs. From our results, this functionalized Co₃O₄@Se NPs/MWCNTs nanocomposite may be considered as a promising candidate for futuristic energy storage and biomedical applications as wearable device.

Research data

It is not relevant to our research work

Data availability

Data will be made available on request.

CRediT authorship contribution statement

Muthukrishnan Francklin Philips and Ragupathy Dhanusuraman: Investigation, Methodology, Validation, Writing - Original draft, Writing - Reviewing and Editing. Jothirathinam Thangarathinam: Supervision. Bavatharani Chokkiah: Writing. Jayakumar Princy: Investigation. Cyril Arockiaraj Crispin Tina: Investigation. Annadurai Kasthuri: Investigation.

CRediT authorship contribution statement

Jothirathinam Thangarathinam: Supervision. Muthukrishnan Francklin Philips: Investigation, Methodology, Validation, Writing – original draft, Writing – review & editing. Violet Dhayabaran: Investigation. Bavatharani Chokkiah: Writing – original draft. Jayakumar Princy: Investigation. Cyril Arockiaraj Crispin Tina: Investigation. Annadurai Kasthuri: Investigation. Ragupathy Dhanusuraman: Investigation, Methodology, Validation, Writing – original draft, Writing – review & editing.

Declaration of Competing Interest

The authors declare that they have no known competing financial interests or personal relationships that could have appeared to influence the work reported in this paper.

Data availability

Data will be made available on request.

Acknowledgements

The authors are grateful to University Grants Commission for funding support (MRP-6651/16 (SERO/UGC). The authors also acknowledged the management of Bishop Heber College (Autonomous), Tiruchirappalli-620017, Tamilnadu, India for the support and facilities rendered through Material Chemistry Lab, P.G. and Research Department of Chemistry and DST-FIST Instrumentation centre (HAIF) for Scientific Instrumentation.

References

- C. Bavatharani, E. Muthusankar, Z.A. Alothman, S.M. Wabaidur, V.K. Ponnusamy, D. Ragupathy, Ultra-high sensitive, selective, non-enzymatic dopamine sensor based on electrochemically active graphene decorated Polydiphenylamine-SiO2 nanohybrid composite, Ceram. Int. 46 (2020) 23276–23281, https://doi.org/ 10.1016/j.ceramint.2020.06.054.
- [2] E. Muthusankar, S.M. Wabaidur, Z.A. Alothman, M.R. Johan, V.K. Ponnusamy, D. Ragupathy, Fabrication of amperometric sensor for glucose detection based on phosphotungstic acid–assisted PDPA/ZnO nanohybrid composite, Ionics (Kiel) 26 (2020) 6341–6349, https://doi.org/10.1007/s11581-020-03740-0.
- [3] B. Chokkiah, M. Eswaran, A.A. Alothman, M. Alsawat, A.A. Ifseisi, K.N. Alqahtani, R. Dhanusuraman, Facile fabrication of hollow polyaniline/carbon nanofibers-coated platinum nanohybrid composite electrode as improved anode electrocatalyst for methanol oxidation, J. Mater. Sci. 33 (2022) 8768–8776, https://doi.org/10.1007/s10854-021-06873-8.
- [4] A. Gopalan, M.F. Philips, J.H. Jeong, K.P. Lee, Synthesis of novel poly(amidoxime) grafted multiwall carbon nanotube gel and uranium adsorption, J. Nanosci. Nanotechnol. 14 (2014) 2451–2458, https://doi.org/10.1166/jnn.2014.8507.
- [5] S.D. Jereil, K. Vijayalakshmi, A. Monamary, Fabrication of highly sensitive MnO2/ F-MWCNT/Ta hybrid nanocomposite sensor with different MnO2 overlayer thickness for H2O2 detection, Ceram. Int. 44 (2018) 8064–8071, https://doi.org/ 10.1016/j.ceramint.2018.01.248.
- [6] M. Azad, Z. Hussain, M.M. Baig, MWCNTs/NiS2 decorated Ni foam based electrode for high-performance supercapacitors, Electrochim. Acta 345 (2020), 136196, https://doi.org/10.1016/j.electacta.2020.136196.
- [7] M. Eswaran, S.M. Wabaidur, Z.A. Alothman, R. Dhanusuraman, V.K. Ponnusamy, Improved cyclic retention and high-performance supercapacitive behavior of poly (diphenylamine-co-aniline)/phosphotungstic acid nanohybrid electrode, Int. J. Energy Res. 45 (2021) 8180–8188, https://doi.org/10.1002/er.5727.
- [8] C. Bavatharani, E. Muthusankar, S.M. Wabaidur, Z.A. Alothman, K.M. Alsheetan, M. mana AL-Anazy, D. Ragupathy, Electrospinning technique for production of polyaniline nanocomposites/nanofibres for multi-functional applications: a review, Synth. Met. 271 (2021), 116609, https://doi.org/10.1016/j.synthmet.2020.116609.
- [9] B. Chokkiah, M. Eswaran, S.M. Wabaidur, Z.A. Alothman, P.C. Tsai, V. K. Ponnusamy, R. Dhanusuraman, Novel PDPA-SiO2 nanosphericals network decorated graphene nanosheets composite coated FTO electrode for efficient electro-oxidation of methanol, Fuel 279 (2020), 118439, https://doi.org/10.1016/i.fuel.2020.118439.
- [10] N. Bhuvanendran, S. Ravichandran, W. Zhang, Q. Ma, Q. Xu, L. Khotseng, H. Su, Highly efficient methanol oxidation on durable PtxIr/MWCNT catalysts for direct methanol fuel cell applications, Int. J. Hydrogen Energy 45 (2020) 6447–6460, https://doi.org/10.1016/j.ijhydene.2019.12.176.
- [11] P. Das, A. Katheria, S. Ghosh, B. Roy, J. Nayak, K. Nath, S. Paul, N. Ch, Self-healable and super-stretchable conductive elastomeric nanocomposites for efficient thermal management characteristics and electromagnetic interference shielding, Synth. Met. 294 (2023), 117304, https://doi.org/10.1016/j.synthmet.2023.117304.
- [12] J. Iqbal, A. Numan, S. Rafique, R. Jafer, S. Mohamad, K. Ramesh, S. Ramesh, High performance supercapattery incorporating ternary nanocomposite of multiwalled carbon nanotubes decorated with Co3O4 nanograins and silver nanoparticles as electrode material, Electrochim. Acta 278 (2018) 72–82, https://doi.org/10.1016/ i.electacta.2018.05.040.
- [13] E. Murugan, G. Vimala, Effective functionalization of multiwalled carbon nanotube with amphiphilic poly(propyleneimine) dendrimer carrying silver nanoparticles for better dispersability and antimicrobial activity, J. Colloid Interface Sci. 357 (2011) 354–365, https://doi.org/10.1016/j.jcis.2011.02.009.
- [14] S. Basu, S. Pande, S. Jana, S. Bolisetty, T. Pal, Controlled interparticle spacing for surface-modified gold nanoparticle aggregates, Langmuir 24 (2008) 5562–5568, https://doi.org/10.1021/la8000784.
- [15] G. Mera, P. Kroll, I. Ponomarev, J. Chen, K. Morita, M. Liesegang, E. Ionescu, A. Navrotsky, Metal-catalyst-free access to multiwalled carbon nanotubes/silica nanocomposites (MWCNT/SiO2) from a single-source precursor, Dalton Trans. 48 (2019) 11018–11033, https://doi.org/10.1039/c9dt01783f.
- [16] M.K. Pitchan, S. Bhowmik, M. Balachandran, M. Abraham, Process optimization of functionalized MWCNT/polyetherimide nanocomposites for aerospace application, Mater. Des. 127 (2017) 193–203, https://doi.org/10.1016/j.matdes.2017.04.081.
- [17] K.M. Manesh, J.H. Kim, P. Santhosh, A.I. Gopalan, K.P. Lee, H.D. Kang, Fabrication of a gold nanoparticles decorated carbon nanotubes based novel modified electrode for the electrochemical detection of glucose, J. Nanosci. Nanotechnol. 7 (2007) 3365–3372, https://doi.org/10.1166/jnn.2007.836.
- [18] M. He, T.M. Swager, Covalent functionalization of carbon nanomaterials with iodonium salts, Chem. Mater. 28 (2016) 8542–8549, https://doi.org/10.1021/acs. chemmater.6b03078.
- [19] N.G. Sahoo, S. Rana, J.W. Cho, L. Li, S.H. Chan, Polymer nanocomposites based on functionalized carbon nanotubes, Progr. Polym. Sci. (Oxford) 35 (2010) 837–867, https://doi.org/10.1016/j.progpolymsci.2010.03.002.
- [20] H. Sadegh, G.A.M. Ali, S. Agarwal, V.K. Gupta, Surface Modification of MWCNTs with Carboxylic-to-Amine and Their Superb Adsorption Performance, Int. J. Environ. Res. 13 (2019) 523–531, https://doi.org/10.1007/s41742-019-00193-w.
- [21] Y.Y. Yilmaz, E.E. Yalcinkaya, D.O. Demirkol, S. Timur, 4-aminothiophenol-intercalated montmorillonite: organic-inorganic hybrid material as an immobilization support for biosensors, Sens. Actuators, B 307 (2020), 127665, https://doi.org/10.1016/j.snb.2020.127665.

- [22] X. Wang, M. Li, Z. Chang, Y. Yang, Y. Wu, X. Liu, Co3O4@MWCNT nanocable as cathode with superior electrochemical performance for supercapacitors, ACS Appl. Mater. Interfaces 7 (2015) 2280–2285, https://doi.org/10.1021/am5062272.
- [23] Y. Fu, J. Jiang, Z. Chen, S. Ying, J. Wang, J. Hu, Rapid and selective removal of Hg (II)ions and high catalytic performance of the spent adsorbent based on functionalized mesoporous silica/poly(m-aminothiophenol)nanocomposite, J. Mol. Liq. 286 (2019), 110746, https://doi.org/10.1016/j.molliq.2019.04.023.
- [24] S. Zeng, Y. Ke, Y. Liu, Y. Shen, L. Zhang, C. Li, A. Liu, L. Shen, X. Hu, H. Wu, W. Wu, Y. Liu, Synthesis and antidiabetic properties of chitosan-stabilized selenium nanoparticles, Colloids Surf. B 170 (2018) 115–121, https://doi.org/10.1016/j.colsurfb.2018.06.003.
- [25] G.M. Neelgund, A. Oki, Deposition of silver nanoparticles on dendrimer functionalized multiwalled carbon nanotubes: synthesis, characterization and antimicrobial activity, J. Nanosci. Nanotechnol. 11 (2011) 3621–3629, https://doi. org/10.1166/jnp.2011.3756.
- [26] K. Chen, Z. Zhang, K. Xia, X. Zhou, Y. Guo, T. Huang, Facile Synthesis of Thiol-Functionalized Magnetic Activated Carbon and Application for the Removal of Mercury(II) from Aqueous Solution, ACS Omega 4 (2019) 8568–8579, https://doi.org/10.1021/acsomega.9b00572.
- [27] P. Boomi, J. Anandha Raj, S.P. Palaniappan, G. Poorani, S. Selvam, H. Gurumallesh Prabu, P. Manisankar, J. Jeyakanthan, V.K. Langeswaran, Improved conductivity and antibacterial activity of poly(2-aminothiophenol)-silver nanocomposite against human pathogens, J. Photochem. Photobiol. B 178 (2018) 323–329, https://doi.org/10.1016/j.jphotobiol.2017.11.029.
- [28] B. Govindaraj, M. Sarojadevi, Microwave-assisted synthesis of nanocomposites from polyimides chemically cross-linked with functionalized carbon nanotubes for aerospace applications, Polym. Adv. Technol. 29 (2018) 1718–1726, https://doi. org/10.1002/pat.4275.
- [29] S. Mallakpour, A. Zadehnazari, Efficient functionalization of multi-walled carbon nanotubes with p-aminophenol and their application in the fabrication of poly (amide-imide)-matrix composites, Polym. Int. 63 (2014) 1203–1211, https://doi. org/10.1002/pi.4622.
- [30] R.M. Obodo, A.C. Nwanya, M. Arshad, C. Iroegbu, I. Ahmad, R.U. Osuji, M. Maaza, F.I. Ezema, Conjugated NiO-ZnO/GO nanocomposite powder for applications in supercapacitor electrodes material, Int. J. Energy Res. 44 (4) (2020) 3192–3202, https://doi.org/10.1002/er.5091.
- [31] B.T. Sone, X.G. Fuku, M. Maaza, Physical & electrochemical properties of green synthesized bunsenite NiO nanoparticles via Callistemon viminalis' extracts, Int. J. Electrochem. Sci. 11 (2016) 8204–8220, https://doi.org/10.20964/2016.10.17.
- [32] S. Khamlich, Z.Y. Nuru, A. Bello, M. Fabiane, J.K. Dangbegnon, N. Manyala, M. Maaza, Pulsed laser deposited Cr2O3 nanostructured thin film on graphene as anode material for lithium-ion batteries, J. Alloys Compd. 637 (2015) 219–225, https://doi.org/10.1016/j.jallcom.2015.02.155.
- [33] R.M. Obodo, N.M. Shinde, U.K. Chime, S. Ezugwu, A.C. Nwanya, I. Ahmad, M. Maaza, P.M. Ejikeme, F.I. Ezema, Recent advances in metal oxide/hydroxide on three-dimensional nickel foam substrate for high performance pseudocapacitive electrodes, Curr. Opin. Electrochem. 21 (2020) 242–249, https://doi.org/10.1016/ i.coelec.2020.02.022.
- [34] M. Hadavifar, N. Bahramifar, H. Younesi, Q. Li, Adsorption of mercury ions from synthetic and real wastewater aqueous solution by functionalized multi-walled carbon nanotube with both amino and thiolated groups, Chem. Eng. J. 237 (2014) 217–228, https://doi.org/10.1016/j.cej.2013.10.014.
- [35] S.A. Gopalan, A.I. Gopalan, A. Vinu, K.P. Lee, S.W. Kang, A new optical-electrical integrated buffer layer design based on gold nanoparticles tethered thiol containing sulfonated polyaniline towards enhancement of solar cell performance, Solar Energy Mater. Solar Cells 174 (2018) 112–123, https://doi.org/10.1016/j. solmat.2017.08.029
- [36] M.R. Nabid, R. Sedghi, A. Bagheri, M. Behbahani, M. Taghizadeh, H. Abdi Oskooie, M.M. Heravi, Preparation and application of poly(2-amino thiophenol)/MWCNTs nanocomposite for adsorption and separation of cadmium and lead ions via solid phase extraction, J. Hazard. Mater. 203–204 (2012) 93–100, https://doi.org/ 10.1016/j.jhazmat.2011.11.096.
- [37] J. Gajendiran, N. Sivakumar, C. Parthasaradhi Reddy, J.R. Ramya, The effect of calcination's temperature on the structural, morphological, optical behaviour, hemocompatibility and antibacterial activity of nanocrystalline Co3O4 powders, Ceram. Int. 46 (2020) 5469–5476, https://doi.org/10.1016/j. ceramint.2019.10.261.
- [38] M.F. Valan, A. Manikandan, S.A. Antony, A novel synthesis and characterization studies of magnetic Co3O4 nanoparticles, J. Nanosci. Nanotechnol. 15 (2015) 4580–4586, https://doi.org/10.1166/jnn.2015.9776.
- [39] M. Bera, C.P. Gupta, P.K. Maji, Facile One-Pot Synthesis of Graphene Oxide by Sonication Assisted Mechanochemical Approach and Its Surface Chemistry, J. Nanosci. Nanotechnol. 18 (2017) 902–912, https://doi.org/10.1166/ inn.2018.14306
- [40] Y. Bai, F. Rong, H. Wang, Y. Zhou, X. Xie, J. Teng, Removal of copper from aqueous solutions by adsorption on elemental selenium nanoparticles, J. Chem. Eng. Data 56 (2011) 2563–2568, https://doi.org/10.1021/je2000777.
- [41] Y.S. Jang, T. Amna, M.S. Hassan, J.L. Gu, I.S. Kim, H.C. Kim, J.H. Kim, S.H. Baik, M.S. Khil, Improved supercapacitor potential and antibacterial activity of bimetallic CNFs-Sn-ZrO2 nanofibers: fabrication and characterization, RSC Adv. 4 (2014) 17268–17273, https://doi.org/10.1039/c3ra47421f.
- [42] B. Chokkiah, M. Eswaran, S.M. Wabaidur, M.R. Khan, V.K. Ponnusamy, D. Ragupathy, A novel electrodeposited poly(melamine)-palladium nanohybrid catalyst on GCE: prosperous multi-functional electrode towards methanol and ethanol oxidation, Fuel 300 (2021), 121005, https://doi.org/10.1016/j. fuel.2021.121005.

- [43] E. Muthusankar, S. Vignesh Kumar, N. Rajagopalan, D. Ragupathy, Synthesis and Characterization of Co-Polymer Nanocomposite Film and its Enhanced Antimicrobial Behavior, Bionanoscience 8 (2018) 1008–1013, https://doi.org/ 10.1007/s12668-018-0564-x.
- [44] P. Kong, R. Wang, C. Zhang, Z. Du, H. Li, W. Zou, Synthesis of 4-aminothiophenol functionalized quantum dots to sensitize silver nanowires and its application for solar cells, Synth. Met. 226 (2017) 50–55, https://doi.org/10.1016/j. cm/htmps/2017.07.004
- [45] C. Zhang, J. Ren, Y. Xing, M. Cui, N. Li, P. Liu, X. Wen, M. Li, Fabrication of hollow ZnO-Co3O4 nanocomposite derived from bimetallic-organic frameworks capped with Pd nanoparticles and MWCNTs for highly sensitive detection of tanshinol drug, Mater. Sci. Eng. C 108 (2020), https://doi.org/10.1016/j. msec.2019.110214.
- [46] S. Chaudhary, S.K. Mehta, Selenium nanomaterials: applications in electronics, catalysis and sensors, J. Nanosci. Nanotechnol. 14 (2014) 1658–1674, https://doi. org/10.1166/jnn.2014.9128.
- [47] Y. Zeng, D.F. Kelley, Surface Charging in CdSe Quantum Dots: infrared and Transient Absorption Spectroscopy, J. Phys. Chem. C 121 (2017) 16657–16664, https://doi.org/10.1021/acs.incc.7b05632.
- [48] V. Krylova, N. Dukstienė, S. Žalenkienė, J. Baltrusaitis, Chemical and structural changes in polyamide based organic-inorganic hybrid materials upon incorporation of SeS 2 O 62– precursor, Appl. Surf. Sci. 392 (2017) 634–641, https://doi.org/10.1016/j.apsusc.2016.09.042.
- [49] K. Kokila, N. Elavarasan, V. Sujatha, Diospyros Montana leaf extract-mediated synthesis of selenium nanoparticles and their biological applications, New J. Chem. 41 (2017) 7481–7490, https://doi.org/10.1039/c7nj01124e.
- [50] D. Maity, C.R. Minitha, R.K. Rajendra, Glucose oxidase immobilized amine terminated multiwall carbon nanotubes/reduced graphene oxide/polyaniline/gold nanoparticles modified screen-printed carbon electrode for highly sensitive amperometric glucose detection, Mater. Sci. Eng. C 105 (2019), 110075, https:// doi.org/10.1016/j.msec.2019.110075.
- [51] R.M. Obodo, A.C. Nwanya, A.B.C. Ekwealor, I. Ahmad, T. Zhao, R.U. Osuji, M. Maaza, F.I. Ezema, Influence of pH and annealing on the optical and electrochemical properties of cobalt (III) oxide (Co3O4) thin films, Surf. Interfaces 16 (2019) 114–119, https://doi.org/10.1016/j.surfin.2019.05.006.
- [52] R.M. Obodo, E.O. Onah, H.E. Nsude, A. Agbogu, A.C. Nwanya, I. Ahmad, T. Zhao, P.M. Ejikeme, M. Maaza, F.I. Ezema, Performance Evaluation of Graphene Oxide Based Co3O4@GO, MnO2@GO and Co3O4/MnO2@GO Electrodes for Supercapacitors, Electroanalysis 32 (2020) 2786–2794, https://doi.org/10.1002/elan.202060262.
- [53] A. Diallo, T.B. Doyle, B.M. Mothudi, E. Manikandan, V. Rajendran, M. Maaza, Magnetic behavior of biosynthesized Co3O4 nanoparticles, J. Magn. Magn. Mater. 424 (2017) 251–255, https://doi.org/10.1016/j.jmmm.2016.10.063.
- [54] A.S. Adekunle, J.A.O. Oyekunle, L.M. Durosinmi, O.S. Oluwafemi, D.S. Olayanju, A.S. Akinola, O.R. Obisesan, O.F. Akinyele, T.A. Ajayeoba, Potential of cobalt and cobalt oxide nanoparticles as nanocatalyst towards dyes degradation in wastewater, Nano-Struct. Nano-Objects 21 (2020), 100405, https://doi.org/10.1016/j.nanoso.2019.100405.
- [55] M.C. Mbambo, M.J. Madito, T. Khamliche, C.B. Mtshali, Z.M. Khumalo, I. G. Madiba, B.M. Mothudi, M. Maaza, Thermal conductivity enhancement in gold decorated graphene nanosheets in ethylene glycol based nanofuid, Sci. Rep. 1 (2020) 14730, https://doi.org/10.1038/s41598-020-71740-1.
- [56] D.P. Sebuso, A.T. Kuvarega, K. Lefatshe, C.K. King'ondu, N. Numan, M. Maaza, C. M. Muiva, Corn husk multilayered graphene/ZnO nanocomposite materials with enhanced photocatalytic activity for organic dyes and doxycycline degradation, Mater. Res. Bull. 151 (2022), 111800, https://doi.org/10.1016/j.materresbull.2022.111800.
- [57] K. Kaviyarasu, E. Manikandan, J. Kennedy, M. Maaza, Synthesis and analytical applications of photoluminescent carbon nanosheet by exfoliation of graphite oxide without purification, J. Mater. Sci. 27 (2016) 13080–13085, https://doi.org/ 10.1007/s10854-016-5451-z.
- [58] T. Kavitha, S. Haider, T. Kamal, M. Ul-Islam, Thermal decomposition of metal complex precursor as route to the synthesis of Co3O4nanoparticles: antibacterial activity and mechanism, J. Alloys Compd. 704 (2017) 296–302, https://doi.org/ 10.1016/j.jallcom.2017.01.306.
- [59] M.K. Uddin, U. Baig, Synthesis of Co3O4 nanoparticles and their performance towards methyl orange dye removal: characterisation, adsorption and response surface methodology, J. Clean. Prod. 211 (2019) 1141–1153, https://doi.org/ 10.1016/j.jclepro.2018.11.232.
- [60] M.C. Mbambo, S. Khamlich, T. Khamliche, M.K. Moodley, K. Kaviyarasu, I. G. Madiba, M.J. Madito, M. Khenfouch, J. Kennedy, M. Henini, E. Manikandan, M. Maaza, Remarkable thermal conductivity enhancement inAg—decorated graphene nanocomposites based nanofuid by laser liquid solid interaction in ethylene glycol, Sci. Rep. 10 (2020) 10982, https://doi.org/10.1038/s41598-020-67418-3
- [61] F.T. Thema, P. Beukes, Z.Y. Nuru, L. Kotsedi, M. Khenfouch, M.S. Dhlamini, B. Juliesc, E. Iwuohah, M. Maaza, Physical properties of graphene via γ-radiolysis of exfoliated graphene oxide, Mater. Today 2 (2015) 4038–4045, https://doi.org/ 10.1016/j.matpr.2015.08.033.
- [62] M. Khenfouch, M. Baïtoul, M. Maaza, White photoluminescence from a grown ZnO nanorods/graphene hybrid nanostructure, Opt. Mater. (Amst.) 34 (2012) 1320–1326, https://doi.org/10.1016/j.optmat.2012.02.005.
- [63] R. Thiramanas, R. Laocharoensuk, Competitive binding of polyethyleneimine-coated gold nanoparticles to enzymes and bacteria: a key mechanism for low-level colorimetric detection of gram-positive and gram-negative bacteria, Microchimica Acta 183 (2016) 389–396, https://doi.org/10.1007/s00604-015-1657-7.

- [64] R. Ahmed, G. Nabi, F. Ali, F. Naseem, M.I. Khan, T. Iqbal, M. Tanveer, Q. Aain, W. Ali, N.S. Arshad, A. Naseem, M. Maraj, M. Shakil, Controlled growth of Mo-Doped NiO nanowires with enhanced electrochemical performance for supercapacitor applications, Mater. Sci. Eng. 284 (2022), 115881, https://doi.org/10.1016/j.mseb.2022.115881.
- [65] X. Zhou, A. Wang, Y. Pan, C. Yu, Y. Zou, Y. Zhou, Q. Chen, S. Wu, Facile synthesis of a Co_3O_4 @carbon, nanotubes/polyindole composite and its application in all-solid-state flexible supercapacitors, J. Mater. Chem. A 3 (2015) 13011–13015, https://doi.org/10.1039/C5TA01906K.
- [66] N.R. Khalid, A. Gull, F. Ali, M.B. Tahir, T. Iqbal, M. Rafique, M.A. Assiri, M. Imran, M. Alzaid, Bi-functional green-synthesis of Co3O4 NPs for photocatalytic and electrochemical applications, Ceram. Int. 48 (2022) 32009–32021, https://doi.org/10.1016/j.ceramint.2022.07.138.
- [67] L. Ding, H. Wang, D. Liu, X.-A. Zeng, Y. Mao, Bacteria capture and inactivation with functionalized multi-walled carbon nanotubes (MWCNTs), J. Nanosci. Nanotechnol. 20 (2019) 2055–2062, https://doi.org/10.1166/jnn.2020.17332.
- [68] Z. Pei, Z. Zhang, G. Li, F. Fu, K. Zhang, Y. Cai, Y. Yang, Improvement of in vitro osteogenesis and antimicrobial activity of injectable brushite for bone repair by incorporating with Se-loaded calcium phosphate, Ceram. Int. 47 (2021) 11144–11155, https://doi.org/10.1016/j.ceramint.2020.12.238.
- [69] D. Hassan, A.T. Khalil, J. Saleem, A. Diallo, S. Khamlich, Z.K. Shinwari, M. Maaza, Biosynthesis of pure hematite phase magnetic iron oxide nanoparticles using floral extracts of Callistemon viminalis (bottlebrush): their physical properties and novel biological applications, Artificial Cells, Nanomed., Biotechnol. 46 (2018) 693–707, https://doi.org/10.1080/21691401.2018.1434534.
- [70] M. Maaza, F. Ezema, J. Kennedy, M. Chaker, A.K.F. Haque, I. Ahmad, M. Akbari, M. Henini, E. Manikandan, K. Bouziane, A. Gibaud, Z. Nuru, R. Obodo, Peculiar

- Size Effects in Nanoscaled Systems, Nano-Horizons (2022), https://doi.org/10.25159/NanoHorizons.9d53e2220e31.
- [71] S.O. Aisida, K. Ugwu, P.A. Akpa, A.C. Nwanya, P.M. Ejikeme, S. Botha, I. Ahmad, M. Maaza, F.I. Ezema, Biogenic synthesis and antibacterial activity of controlled silver nanoparticles using an extract of Gongronema Latifolium, Mater. Chem. Phys. 237 (2019), 121859, https://doi.org/10.1016/j.matchemphys.2019.121859.
- [72] D. Havenga, R. Akoba, L. Menzi, S. Azizi, J. Sackey, N. Swanepoel, A. Gibaud, M. Maaza, From Himba indigenous knowledge to engineered Fe₂O₃ UV-blocking green nanocosmetics, Sci. Rep. 12 (2022) 2259, https://doi.org/10.1038/s41598-021-04663-0.
- [73] N. Ditlopo, N. Sintwa, S. Khamlich, E. Manikandan, K. Gnanasekaran, M. Henini, A. Gibaud, A. Krief, M. Maaza, From Khoi-San indigenous knowledge to bioengineered CeO2 nanocrystals to exceptional UV-blocking green nanocosmetics, Sci. Rep. 12 (2022) 3468, https://doi.org/10.1038/s41598-022-06838 r.
- [74] H. Zhang, H. Zhou, J. Bai, Y. Li, J. Yang, Q. Ma, Y. Qu, Biosynthesis of selenium nanoparticles mediated by fungus Mariannaea sp. HJ and their characterization, Colloids Surf. A 571 (2019) 9–16, https://doi.org/10.1016/j.colsurfa.2019.02.070.
- [75] H.Y. Mostafa, G.S. El-Sayyad, H.G. Nada, R.A. Ellethy, E.G. Zaki, Promising antimicrobial and antibiofilm activities of Orobanche aegyptiaca extract-mediated bimetallic silver-selenium nanoparticles synthesis: effect of UV-exposure, bacterial membrane leakage reaction mechanism, and kinetic study, Arch. Biochem. Biophys. 736 (2023), 109539, https://doi.org/10.1016/j.abb.2023.109539.
- [76] F. Gao, B. Ma, Z. She, Y. Zhao, L. Guo, C. Jin, M. Gao, Performance evaluation, enzymatic activity and microbial community of sequencing batch reactor under hydroxyl-functionalized multi-walled carbon nanotubes (MWCNTs-OH) stress, Environ. Technol. Innov. 21 (2021), 101213, https://doi.org/10.1016/j. eti.2020.101213.